

**Manuscript version: Author's Accepted Manuscript**

The version presented in WRAP is the author's accepted manuscript and may differ from the published version or Version of Record.

**Persistent WRAP URL:**

<http://wrap.warwick.ac.uk/114217>

**How to cite:**

Please refer to published version for the most recent bibliographic citation information. If a published version is known of, the repository item page linked to above, will contain details on accessing it.

**Copyright and reuse:**

The Warwick Research Archive Portal (WRAP) makes this work by researchers of the University of Warwick available open access under the following conditions.

© 2017 Elsevier. Licensed under the Creative Commons Attribution-NonCommercial-NoDerivatives 4.0 International <http://creativecommons.org/licenses/by-nc-nd/4.0/>.



**Publisher's statement:**

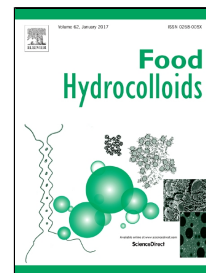
Please refer to the repository item page, publisher's statement section, for further information.

For more information, please contact the WRAP Team at: [wrap@warwick.ac.uk](mailto:wrap@warwick.ac.uk).

# Accepted Manuscript

Shear degradation of corn starches with different amylose contents

Xingxun Liu, Xiaoming Xiao, Peng Liu, Long Yu, Ming Li, Sumei Zhou, Fengwei Xie



PII: S0268-005X(16)30845-1

DOI: [10.1016/j.foodhyd.2016.11.023](https://doi.org/10.1016/j.foodhyd.2016.11.023)

Reference: FOOHYD 3684

To appear in: *Food Hydrocolloids*

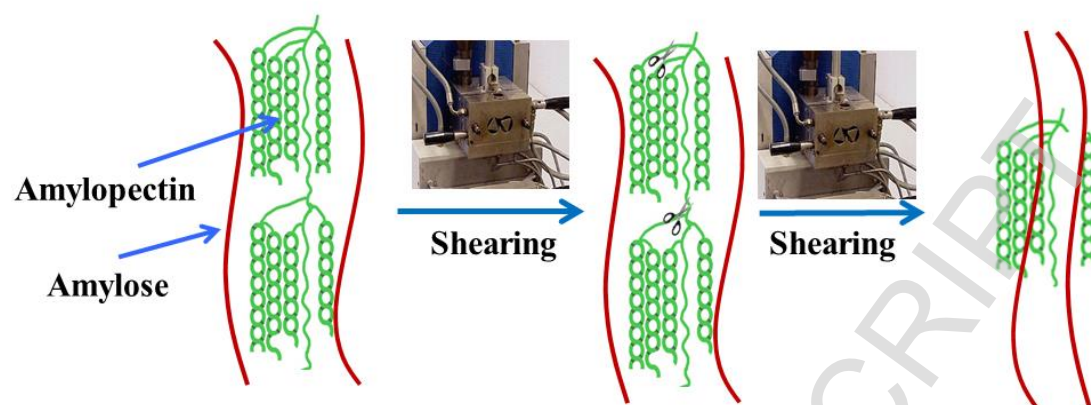
Received Date: 19 August 2016

Revised Date: 14 November 2016

Accepted Date: 18 November 2016

Please cite this article as: Xingxun Liu, Xiaoming Xiao, Peng Liu, Long Yu, Ming Li, Sumei Zhou, Fengwei Xie, Shear degradation of corn starches with different amylose contents, *Food Hydrocolloids* (2016), doi: 10.1016/j.foodhyd.2016.11.023

This is a PDF file of an unedited manuscript that has been accepted for publication. As a service to our customers we are providing this early version of the manuscript. The manuscript will undergo copyediting, typesetting, and review of the resulting proof before it is published in its final form. Please note that during the production process errors may be discovered which could affect the content, and all legal disclaimers that apply to the journal pertain.

**Graphical abstract**

## Highlights

- ✓ Starch structural changes under shear was studied using SEC and SAXS
- ✓ Amylopectin molecules degraded to a stable size under shear
- ✓ Shear disrupted the starch lamellar structure effectively
- ✓ Higher-amylopectin starch was more prone to granule damage

## Shear degradation of corn starches with different amylose contents

Xingxun Liu<sup>a,\*</sup>, Xiaoming Xiao<sup>b</sup>, Peng Liu<sup>c</sup>, Long Yu<sup>b</sup>, Ming Li<sup>a</sup>, Sumei Zhou<sup>a</sup>, Fengwei Xie<sup>d,\*\*</sup>

<sup>a</sup> Institute of Food Science and Technology (IFST), Chinese Academy of Agricultural Science (CAAS), Beijing, 100193, China

<sup>b</sup> School of Food Science and Engineering, South China University of Technology (SCUT), Guangzhou, 510640, China

<sup>c</sup> School of Chemistry and Chemical Engineering, Guangzhou University, Guangzhou, 510006, China

<sup>d</sup> School of Chemical Engineering, The University of Queensland, Brisbane, Qld 4072, Australia

\* Corresponding author at: Institute of Food Science and Technology, CAAS, Beijing, China. *E-mail:* [ytboy652@163.com](mailto:ytboy652@163.com) (X. Liu).

\*\* Corresponding author at: School of Chemical Engineering, The University of Queensland, Brisbane, Qld 4072, Australia. *Email:* [f.xie@uq.edu.au](mailto:f.xie@uq.edu.au), [fwhsieh@gmail.com](mailto:fwhsieh@gmail.com) (F. Xie)

**Abstract:** This work investigated the effect of shear on the starch degradation, with a particular focus on the changes in molecular and lamellar structures. Corn starches with different amylose/amylopectin ratios (waxy corn starch, or WCS: 1:99; normal corn starch, or NCS: 25:75; and Gelose 80 starch, or G80: 80:20) were used as model materials to be processed using a Haake twin-rotor mixer for different times. Molecular and lamellar structural analysis was performed using size-exclusion chromatography (SEC) and small-angle X-ray scattering (SAXS). The degree of damage of starch at the granule level was evaluated by an assay kit. The results showed that amylose molecules in starch granules did not change significantly, while amylopectin molecules degraded to a stable size caused by the shear treatment. The average thickness of semi-crystalline lamellae disappeared rapidly during processing. A typical positive deviation from Porod's law at a high  $q$  region was observed, attributed to the presence of thermal density fluctuations or mixing within phases. Nonetheless, the degree of mixing within phases for the processed samples was lower than the native starch. The study of the mass fractal structure indicated that the scattering objects of the processed starches were more compact than those of the native counterparts. Furthermore, waxy corn starch (containing mostly amylopectin) experienced the greatest granule damage than the other starches. All the results showed that the rigid crystal structure in amylopectin is more sensitive to the shear treatment than the flexible amorphous structure in amylose. This mechanistic understanding at the microstructure level is helpful in designing the processing of starch-based foods or plastics with desired functional properties.

**Keywords:** starch, degradation, shear strength, amylose, lamellar structure

## 1. Introduction

Starch is the main component of cereal-based foods, which is a primary source of energy for humans. Besides, due to its total biodegradability, low cost, and wider availability, starch has attracted much attention as an important raw material for producing biodegradable plastics to replace some petroleum-based polymers (Yu, Dean, & Li, 2006). Extrusion is commonly used in industry for the processing of starch-based foods and materials. Gelatinization and degradation are two most important phenomena in extrusion processing, affecting the material performance (Liu et al., 2013). Starch degradation during processing has shown to be strongly correlated to the mechanical properties of starch-based materials (Liu, Halley, & Gilbert, 2010; Li, Hasjim, Xie, Halley, & Gilbert, 2014).

It is well known that the multi-scale structure of the starch granule is mainly composed of amylose and amylopectin. These two macromolecules are the basis of the aggregation and granule structure of starch and provide an excellent conceptual approach to the understanding of the structure-processing-property relationships of natural polymers (Pérez & Bertoft, 2010; Wu, Witt, & Gilbert, 2013; Liao, Liu, Liu, Lin, Yu, & Chen, 2014). Amylose is a linear molecular with a few long branches, whereas amylopectin is highly branched, containing ~5% branching points and a large number of short branches (Damager, Engelsens, Blennow, Lindberg Møller, & Motawia, 2010; Pérez et al., 2010). The outer parts of amylopectin branches (A and B<sub>1</sub> chains) form clusters of double helices, which build up the crystalline lamellae; and the internal parts (B<sub>2</sub>, B<sub>3</sub> and C chains) locate in the amorphous lamellae (Jane, Xu, Radosavljevic, & Seib, 1992). The alternating crystalline and amorphous lamellae with a ~9 nm repeat distance collectively form the semi-crystalline growth rings in a starch granule (Calvert, 1997; Damager et al., 2010). Amylose is in either amorphous or single

helical conformation and is interspersed among amylopectin molecules (Jane et al., 1992; Lopez-Rubio, Flanagan, Gilbert, & Gidley, 2008).

The mechanical shear in extrusion processing induces gelatinization, with the breakage of the crystalline structure of starch (Xie, Halley, & Avérous). This process is entirely different from the usual gelatinization process under heat-moisture treatment (Zhang, Chen, Liu, & Wang, 2010) or annealing (Liu, Yu, Simon, Dean, & Chen, 2009). In our previous paper, the lamellar structure of starch during gelatinization process was studied by synchrotron-SAXS/WAXS (Zhang et al., 2015; Kuang et al., 2016). It was observed that, before the gelatinization temperature, the lamellar peak intensity decreased, and the thickness of crystalline lamellae increased, whereas the size of both amorphous and crystallinity lamellae disappeared rapidly around the gelatinization temperature. However, there have been no comprehensive studies on the change of starch lamellar structure under shear treatment.

On the other hand, shear may also induce the change in the molecular size of starch. Liu et al. (2010) and Li et al. (2014) have used size-exclusion chromatography (SEC) to investigate the degradation mechanism of corn starch during extrusion. They found that the mechanical energy played a dominant role in reducing the starch molecular size, and amylopectin in starch granules was more susceptible to shear degradation than amylose. However, as extrusion is a process involving a complex flow and multiple temperature sections, it is difficult to obtain a precise understanding of the relationship between processing conditions and the resultant structure of starch.

Recently, an internal twin-rotor mixer has been used to understand the gelatinization (Xue, Yu, Xie, Chen, & Li, 2008; Wang, Yu, Xie, Chen, Li, & Liu, 2010) and chemical modification (Qiao et al., 2012; Qiao, Bao, Liu, Chen, Zhang, & Chen, 2014) of starch during processing. A HAAKE



Rheomix twin-rotor mixer can not only be used a processing device, but also serves as a rheometer to accurately monitoring the processing conditions (Yang, Bigio, & Smith, 1995). This device can represent a short section of an extruder so it could be useful to understand the processing-structure relationship in a simpler manner. Yet, the change of the multi-level starch structure during kneading using a twin-rotor mixer has not been reported.

In this study, corn starches with different amylose/amylopectin ratios were used as model materials to reveal the shear-induced starch degradation during kneading. The molecular and lamellar structures were studied by SEC and small-angle X-ray scattering (SAXS), respectively. The information obtained from this study would help to understand the shear degradation mechanism and to design new starch materials with accurately-controlled structures.

## 2. Material and Method

### 2.1 Sample and sample prepared

Commercially-available corn starches with different amylose contents were used in this experimental work. Waxy corn starch (WCS) (1% amylose content) was supplied by Lihua Starch Industry Co., Ltd.. Normal corn starch (NCS) (25% amylose content) was provided by Huanglong Food Industry Co., Ltd.. Gelose 80 starch (G80) (80% amylose content) was supplied by National Starch Pty Ltd. (Lane Cove, NSW 2066, Australia).

Starch and water were pre-mixed in a high-speed mixer (capacity 10 L, SRLW 10/25, Fanchang machinery Co. LCD, China) at 1000 rpm for 5 min. An infrared heating balance (Model DHS-20, Longway & Yueping, Shanghai, China) was used to measure the moisture content during

heating the sample to 110 °C for 20 min. The total moisture content (about 35%) of a specimen was taken as the sum of the original starch moisture content and the added water.

## 2.2 Haake rheometer

A Haake Rheocord PolyLab RC500p system incorporating a HAAKE Rheomix 600p twin-rotor mixer (ThermoHaake, Germany) was used in the experimental work. This equipment was described in detail previously (Xue et al., 2008; Wang et al., 2010). The material was introduced into the mixer through a top-mounted loading hopper, and torque and temperature were recorded immediately after loading. The roller speed of 75 rpm and initial temperatures 70 °C were used. The samples were collected at different times (0, 2, 5, 7, 10 and 15 min) and ground into power using a cryo-grinder (ZM200, Retsch) under liquid nitrogen for further analysis.

## 2.3 Size-exclusion chromatography

The molecular size and size distribution of fully-branched and debranched starch molecules were measured using size-exclusion chromatography (SEC) (Tran, Shelat, Tang, Li, Gilbert, & Hasjim, 2011). The extracted native starch granules (about 6 mg) were dissolved in DMSO/LiBr solution and then debranched using isoamylase in acetate buffer (pH ~3.5), following the method of Li, Hasjim, Dhital, Godwin, and Gilbert (2011). Then, the weight size distributions of fully-branched and debranched starch molecules were analyzed in duplicate using SEC (Agilent 1260 series, Agilent Technologies, Santa Clara, California, USA) equipped with a refractive index detector (Optilab T-rEX, WYATT Corp., USA). The injection volume was 100 µL, the flow rate was 0.3 mL/min, and the column oven temperature was at 80 °C. A series of columns (GRAM precolumn, GRAM 30, and

GRAM 3000 analytical columns, Polymer Standard Services, Mainz, Germany) were used to analyze the size distribution of fully-branched starch molecules. Another series of columns (GRAM precolumn, GRAM 100, and GRAM 1000 analytical columns, Polymer Standard Services, Mainz, Germany) were used to analyze the size distribution of debranched starch molecules. A series of pullulan standards (Polymer Standard Services, Mainz, Germany) with varying molecular weights ranging from 342 to  $2.35 \times 10^6$  Da were used for calibration to obtain the relationship between the SEC elution volume and the hydrodynamic volume  $V_h$  (which is the separation parameter for SEC). Data are presented as the SEC weight distribution,  $w(\log V_h)$ , as a function of the corresponding hydrodynamic radius  $R_h$ , with  $V_h = (4/3)\pi R_h^3$ . Because the largest standard had a hydrodynamic radius of  $\sim 50$  nm, this is the maximum size at which calibration is reliable. The dependence of  $R_h$  on elution volume for larger sizes was obtained by extrapolation of the calibration curve and thus are only semi-quantitative, and also sensitive to day-to-day variations (Wang, Hasjim, Wu, Henry, & Gilbert, 2014).

#### 2.4 Small-angle X-ray scattering (SAXS)

Synchrotron small-angle X-ray scattering (SAXS) measurements were carried out at the BL16B1 beamline at the Shanghai Synchrotron Radiation Facility (SSRF), China. Distilled water was added to the starch in a glass vial to obtain a starch suspension with the starch:water ratio being 1:3 (w/v). The suspension was equilibrated for 24 h before SAXS tests. Then, the starch suspension (0.70 mL) was loaded into a 2-mm-thick sample cell, of which both the front and back windows were covered with the Kapton tape. Two-dimensional (2D) Mar165 were used to collect the 2D SAXS patterns. The wavelength of the incident X-ray was 1.24 Å, and the sample-to-detector

distance (SDD) was 1940 mm for SAXS measurements. A beef tendon specimen was used as standard materials for the calibration of the scattering vector of SAXS. By measuring sample adsorption using the ionization chambers in the front and back of the sample cell, we performed data correction, calibrated the SAXS data from the background scattering, and normalized the data on the primary beam intensity. Background subtraction follows the equation:

$$I_s(\theta) = I_t(\theta) - \frac{I_t T_t}{I_b T_b} I_b(\theta).$$

$I_t(\theta)$ ,  $I_b(\theta)$  and  $I_s(\theta)$  represent the distribution of scattering intensity of samples held in cells, sample cells and pure samples, respectively.  $I_t$  and  $I_b$  represent values of samples held in the cells and sample cells, read from the ionization chambers in front of sample cell.  $T_t$  and  $T_b$  represent the transmissivity of the samples held in cells and sample cells.

## 2.5 Damage of starch granules

The degree of damage to starch granules was determined according to the AACC method 76-31.01 using an assay kit from Megazyme International Ltd. (Ireland) (AACC International Method 76-31.01). The tests were based on the susceptibility to amylolytic enzyme hydrolysis, using the Megazyme starch damage assay kit in triplicate, following the procedure provided by the manufacturer (AACC International Method 76-13.01).

## 3. Result and Discussion

### 3.1 Shear behavior of starch

The Haake rheometer with a twin-roll mixer can be used not only for melting and blending of polymers (Liu, Wang, Chow, Yang, & Mitchell, 2014), but also provides information on torque

variation during the kneading process. Fig. 1 shows a typical curve of torque variation with time for a starch during kneading. The peak (a) occurred during the loading due to the resistance force when the cold materials were rapidly loaded into the mixer. After the loading of material, the torque decreased, and then increased to form a broad peak (b), representing the maximum viscosity resulting from the granule swelling and gelatinization. After the second peak (b), more starch granules were destroyed, resulting in a decreasing torque (c) until the end of the measurement (20 min), with the gradually-reduced decrease rate (d). Moreover, the temperature increased gradually with time, resulting in the reduction in viscosity and torque.

In our previous paper (Xue et al., 2008; Wang et al., 2010), the effects of water content, rotor speed and initial temperature on the torque and temperature have been studied. The results showed that the starch granules first swelled and then disintegrated, and finally all the granules were destroyed. Microscopy and DSC confirmed that the semi-crystallinity structure of starch granules was destroyed by the shear stress.

### 3.2 Molecular size distribution of fully branched starch during shear

Although DSC and polarized-light microscopy can detect the crystal structure change during the kneading process, the change of starch molecular structure (such as size and size distribution) is still unclear. Fig. 2 shows weight distributions of the whole (fully-branched) starch molecules collected at different kneading times by SEC. All the weight distributions of the whole starch molecules were normalized to the highest peak. For NCS, two peaks were observed from SEC. One peak ( $R_h = \sim 10$  nm) was due to amylose, and the other ( $R_h = \sim 100$  nm) was due to amylopectin (Liu et al., 2010; Tran et al., 2011; Li et al., 2014).

The amylopectin peak area for NCS and WCS became smaller and amylose peak area became larger during kneading compared with their native counterparts. However, the value did not change significantly for G80, which may relate to its more intact granule (Li et al., 2014). From Fig. 2, it was clearly seen that the amylose/amylopectin ratio also affected the degradation mechanism of starch. The amylopectin molecule was easier to degrade than amylose during kneading. For the degraded amylopectin molecules (WCS), a new peak ( $R_h \approx 50$  nm) representing the stable size achieved during kneading could be identified. The shear-induced molecular size reduction to a stable value has also been reported previously (Liu et al., 2010; Li et al., 2014). For NCS, the size of amylopectin molecules decreased with time and showed a stable size of 50 nm. For amylose molecules (G80), the highest value of  $R_h$  was about 10 nm from the whole molecules SEC weight distributions, which was smaller than the stable size for WCS and NCS. This difference might be due to the smaller size of the amylose in G80.

### 3.3 Molecular size distribution of debranched starch during shear

Typical SEC weight distributions of debranched starch molecules are shown in Fig. 3. For NCS, a bi-modal peak was observed which was associated with the amylopectin branches ( $R_h < 4$  nm) and there was a broader bi-modal peak, which was associated with the amylose branches ( $R_h > 4$  nm) (Tran et al., 2011). Besides, there was a shoulder peak at about  $R_h \approx 2$  nm representing the B<sub>2</sub>, B<sub>3</sub> chains in amylopectin branches, which spans more than one lamella. In Fig. 3, there were no qualitative differences in the weight distributions of the debranched starch between NCS and its processed samples collected at different times. The results indicated that the glycosidic bonds near or at the branching points, sometimes termed building blocks (Dhital, Shrestha, & Gidley, 2010), of the

amylopectin molecules, were susceptible to shear degradation during the melting kneading process. WCS and G80 showed similar results in this study.

### 3.4 Lamellar structure change during shear

The SAXS one-dimensional (1D) scattering intensity distributions for starches with different amylose content are shown in Fig. 4. A clear lamellar peak at  $q = \sim 0.68 \text{ nm}^{-1}$  was observed in SAXS curves of native starches, which was corresponding to the 9–10 nm semi-crystalline lamellar structure of starch (Chen, Wang, Kuang, Zhou, Wang, & Liu, 2016). From Fig. 4, it can be clearly seen that the scattering intensity of the lamellar peak for the amylopectin-rich starch was higher than the amylose-rich starch, indicating a higher electron density contrast ( $\Delta\rho = \rho_c - \rho_a$ , where  $\rho_c$  and  $\rho_a$  are the electron densities of the crystalline regions and the amorphous regions in the semi-crystalline lamellae) between crystalline and amorphous lamellae.

It could also be clearly seen in Fig. 4 that the lamellar peak disappeared rapidly (as early as 2 min), which meant that the crystalline lamellar structure was damaged by shear. The kneading process is different from a general gelatinization process where heating (Vermeulen, Derycke, Delcour, Goderis, Reynaers, & Koch, 2006; Zhang et al., 2015), microwave heating (Fan et al., 2013; Fan et al., 2014), or ultra-high hydrostatic pressure (Yang, Gu, Lam, Tian, Chaieb, & Hemar, 2016a) was applied. The *in-situ* SAXS data showed that the change under mechanical kneading was a more gradual process. The crystalline lamellar size of starch obtained from the correlation function was increased even before the gelatinization temperature. The twin-rotor mixer would provide the shear energy to destroy the starch granules structure. The rigid crystallites in starch granules were mainly formed by amylopectin and these crystallites were most susceptible to shear, as seen from the SEC

results showing the decrease in the size of amylopectin. The destruction to the amylopectin crystallites was proposed to lead to the disappearance of the lamellar peak.

### 3.5 Mixing within phase and fractal dimension of starch granule

It is well known that only the scattering by an ideal two-phase system with sharp boundaries obeys Porod's law (Li et al., 2001). However, deviation from this law is often observed in practice. A negative deviation is due to the finite diffuse-boundary thickness between two phases and a positive deviation due to the density fluctuation resulting from either the movement of electrons or compositional heterogeneity within scattering elements (Xu et al., 2004). In this study, the  $\ln(I \times q^4) \sim q^2$  patterns of the starch treated in the mixer are shown in Fig. 5. All the starch samples showed a typical positive deviation from Porod's law at a high  $q$  region, which could be attributed to the presence of thermal density fluctuations or mixing within phases (Yang et al., 2016a; Yang et al., 2016b). In the current work, the mixing of the starch was that between crystalline and amorphous phases. Compared to the native starch, the treated starch displayed a reduced slope, suggesting the degree of mixing within phases was lower than the native starch.

The fractal dimension from SAXS data can be used to describe the self-similar structure of starch granules in a given region (Suzuki, Chiba, & Yano, 1997), which means the structure is independent of the observation scale. The fractal dimension helps to quantify the compactness properties such as mass ( $m$ ) and surface area ( $A$ ). The slope ( $-\alpha$ ) of  $\log I(q)$  vs.  $\log q$  curves in the linear region was calculated, with linear regression analysis, leading to fractal dimensions ( $D_f$ ). For  $\alpha$  between 1 and 3,  $D_f$  equals  $\alpha$  and the material is characterized as mass fractal ( $D_m$ ) in a three-



dimensional space (Leite et al., 2007). These parameters could indicate if the density profile of the scattering objects has a self-similar nature.

The length scale for  $D_f$  ranging from 1 to 3 for all corn starches with different mixing time is between 32 nm and 57 nm, suggesting the presence of a mass fractal structure in starch granules. However, the value for the shear-treated starch was lower than the native starch, which meant that the scattering objects in the treated starch were more compact.

### 3.6 Degree of damage of starch granules

Mechanical kneading can damage starch granules to some extent, which significantly influence the physicochemical properties of starch. The damage to the starch granules in the mixer (see Table 1) increased significantly from about 0 to over 20%, even 40% for WCS. Moreover, the degree of damage for WCS was higher than that for G80, which also suggested that WCS was more fragile. The different susceptibility of various starches was also observed using lab-scale ball milling (Tester, 1997). The degrees of damage of starches detected here were in agreement with our previous paper (Wang et al., 2010). Overall, the starch with higher amylose content was more resistant to external physical treatment.

## 4. Conclusion

The structural changes of corn starches with different amylose contents during kneading using a twin-rotor mixer were investigated. Resulting from kneading, no apparent changes were observed for the amylose molecules in starch granules, while amylopectin molecules degraded to a stable size during the processing. The lamellar peak, which represents the average thickness of semi-

crystalline lamellae disappeared rapidly during mixing. A typical positive deviation from Porod's law at a high  $q$  region was observed, which was attributed to the presence of thermal density fluctuations or mixing within phases. The degrees of mixing within phases for the processed starches were lower than for the native counterparts. The mass fractal values indicated that the scattering objects of the processed starch were more compact. Moreover, the degree of damage of WCS was higher than those of the other two starches. All the results showed that the rigid crystallites of amylopectin in starch granules were more susceptible to shear degradation compared with the flexible amorphous amylose. The starch degradation mechanism, concluded from the present study, is similar to the dry grinding mechanism of starch granules at a cryogenic temperature. This mechanistic understanding from the characterizations of different starch structural levels is helpful in designing the processing of starch-based foods and plastics with desired structure and improved functional properties.

## Conflict of interest

The authors declare that there is no conflict of interests regarding the publication of this paper.

## Acknowledgments

The authors from China would like to acknowledge the research funds NFSC (Nos. 31301554 and 31571789).

## References

- AACC International. Approved Methods of Analysis, 11th Ed. Method 76-31.01. Determination of damaged starch. Spectrophotometric method. Approved November 3rd, 1999. AACC International, St Paul, MN.
- Calvert, P. (1997). Biopolymers: The structure of starch. *Nature*, 389, 338-339.
- Chen, P., Wang, K., Kuang, Q., Zhou, S., Wang, D., & Liu, X. (2016). Understanding how the aggregation structure of starch affects its gastrointestinal digestion rate and extent. *International Journal of Biological Macromolecules*, 87, 28-33.
- Damager, I., Engelsen, S. B., Blennow, A., Lindberg Møller, B., & Motawia, M. S. (2010). First principles insight into the  $\alpha$ -glucan structures of starch: Their synthesis, conformation, and hydration. *Chemical Reviews*, 110, 2049-2080.
- Dhital, S., Shrestha, A. K., & Gidley, M. J. (2010). Effect of cryo-milling on starches: Functionality and digestibility. *Food Hydrocolloids*, 24, 152-163.
- Fan, D., Wang, L., Chen, W., Ma, S., Ma, W., Liu, X., Zhao, J., & Zhang, H. (2014). Effect of microwave on lamellar parameters of rice starch through small-angle x-ray scattering. *Food Hydrocolloids*, 35, 620-626.
- Fan, D., Wang, L., Ma, S., Ma, W., Liu, X., Huang, J., Zhao, J., Zhang, H., & Chen, W. (2013). Structural variation of rice starch in response to temperature during microwave heating before gelatinisation. *Carbohydrate Polymers*, 92, 1249-1255.
- International, A. *Aacc international method 76-13.01, total starch assay procedure (megazyme amyloglucosidase/ $\alpha$ -amylase method). First approval november 8, 1995; reapproval november 3, 1999.* . AACC International, St. Paul, MN, U.S.A.
- International, A. *Aacc international method 76-31.01, determination of damaged starch - spectrophotometric method. Final approval november 8, 1995; reapproval november 3, 1999.* St. Paul, MN, U.S.A.: AACC International.
- Jane, J., Xu, A., Radosavljevic, M., & Seib, P. A. (1992). Location of amylose in normal starch granules. I. Susceptibility of amylose and amylopectin to cross-linking reagents. *Cereal Chemistry*, 69, 405-409
- Kuang, Q., Xu, J., Liang, Y., Xie, F., Tian, F., Zhou, S., & Liu, X. (2016). Lamellar structure change of waxy corn starch during gelatinization by time-resolved synchrotron saxs. *Food Hydrocolloids*.
- Leite, F. L., de Oliveira Neto, M., Paterno, L. G., Ballesterro, M. R. M., Polikarpov, I., Mascarenhas, Y. P., Herrmann, P. S. P., Mattoso, L. H. C., & Oliveira Jr, O. N. (2007). Nanoscale conformational ordering in polyanilines investigated by saxs and afm. *Journal of Colloid and Interface Science*, 316, 376-387.
- Li, E., Hasjim, J., Dhital, S., Godwin, I. D., & Gilbert, R. G. (2011). Effect of a gibberellin-biosynthesis inhibitor treatment on the physicochemical properties of sorghum starch. *Journal of Cereal Science*, 53, 328-334.
- Li, M., Hasjim, J., Xie, F., Halley, P. J., & Gilbert, R. G. (2014). Shear degradation of molecular, crystalline, and granular structures of starch during extrusion. *Starch - Stärke*, 66, 595-605.
- Li, Z. H., Gong, Y. J., Wu, D., Sun, Y. H., Wang, J., Liu, Y., & Dong, B. Z. (2001). A negative deviation from porod's law in saxs of organo-msu-x. *Microporous and Mesoporous Materials*, 46, 75-80.
- Liao, L., Liu, H., Liu, X., Lin, Yu, L., & Chen, P. (2014). Development of microstructures and phase transitions of starch. *Acta Polym Sinica*, 21, 761-773.
- Liu, H. S., Yu, L., Simon, G., Dean, K., & Chen, L. (2009). Effects of annealing on gelatinization and microstructures of corn starches with different amylose/amylopectin ratios. *Carbohydr Polym*, 77, 662-669.
- Liu, W.-C., Halley, P. J., & Gilbert, R. G. (2010). Mechanism of degradation of starch, a highly branched polymer, during extrusion. *Macromolecules*, 43, 2855-2864.
- Liu, X., Wang, T., Chow, L. C., Yang, M., & Mitchell, J. W. (2014). Effects of inorganic fillers on the thermal and mechanical properties of poly (lactic acid). *International Journal of Polymer Science*.

- 343 Liu, X., Wang, Y., Yu, L., Tong, Z., Chen, L., Liu, H., & Li, X. (2013). Thermal degradation and stability of starch under  
344 different processing conditions. *Starch - Stärke*, 65, 48-60.
- 345 Lopez-Rubio, A., Flanagan, B. M., Gilbert, E. P., & Gidley, M. J. (2008). A novel approach for calculating starch  
346 crystallinity and its correlation with double helix content: A combined xrd and nmr study. *Biopolymers*, 89,  
347 761-768.
- 348 Pérez, S., & Bertoft, E. (2010). The molecular structures of starch components and their contribution to the architecture  
349 of starch granules: A comprehensive review. *Starch - Stärke*, 62, 389-420.
- 350 Qiao, D.-l., Bao, X.-y., Liu, X.-x., Chen, L., Zhang, X.-q., & Chen, P. (2014). Preparation of cassava starch-based  
351 superabsorbent polymer using a twin-roll mixer as reactor. *Chinese Journal of Polymer Science*, 32, 1348-1356.
- 352 Qiao, D., Zou, W., Liu, X., Yu, L., Chen, L., Liu, H., & Zhang, N. (2012). Starch modification using a twin - roll mixer as a  
353 reactor. *Starch - Stärke*, 64, 821-825.
- 354 Suzuki, T., Chiba, A., & Yarno, T. (1997). Interpretation of small angle x-ray scattering from starch on the basis of  
355 fractals. *Carbohydrate Polymers*, 34, 357-363.
- 356 Tester, R. F. (1997). Properties of damaged starch granules: Composition and swelling properties of maize, rice, pea and  
357 potato starch fractions in water at various temperatures. *Food Hydrocolloids*, 11, 293-301.
- 358 Tran, T. T. B., Shelat, K. J., Tang, D., Li, E., Gilbert, R. G., & Hasjim, J. (2011). Milling of rice grains. The degradation on  
359 three structural levels of starch in rice flour can be independently controlled during grinding. *Journal of*  
360 *Agricultural and Food Chemistry*, 59, 3964-3973.
- 361 Vermeylen, R., Derycke, V., Delcour, J. A., Goderis, B., Reynaers, H., & Koch, M. H. J. (2006). Gelatinization of starch in  
362 excess water: Beyond the melting of lamellar crystallites. A combined wide- and small-angle x-ray scattering  
363 study. *Biomacromolecules*, 7, 2624-2630.
- 364 Wang, J., Yu, L., Xie, F., Chen, L., Li, X., & Liu, H. (2010). Rheological properties and phase transition of cornstarches with  
365 different amylose/amylopectin ratios under shear stress. *Starch - Stärke*, 62, 667-675.
- 366 Wang, K., Hasjim, J., Wu, A. C., Henry, R. J., & Gilbert, R. G. (2014). Variation in amylose fine structure of starches from  
367 different botanical sources. *Journal of Agricultural and Food Chemistry*, 62, 4443-4453.
- 368 Wu, A. C., Witt, T., & Gilbert, R. G. (2013). Characterization methods for starch-based materials: State of the art and  
369 perspectives. *Australian Journal of Chemistry*, 66, 1550-1563.
- 370 Xie, F., Halley, P. J., & Avérous, L. Rheology to understand and optimize processability, structures and properties of  
371 starch polymeric materials. *Progress in Polymer Science*.
- 372 Xu, Y., Li, Z., Fan, W., Wu, D., Sun, Y., Rong, L., & Dong, B. (2004). Density fluctuation in silica-pva hybrid gels  
373 determined by small-angle x-ray scattering. *Applied Surface Science*, 225, 116-123.
- 374 Xue, T., Yu, L., Xie, F. W., Chen, L., & Li, L. (2008). Rheological properties and phase transition of starch under shear  
375 stress. *Food Hydrocolloids*, 22, 973-978.
- 376 Yang, L.-Y., Bigio, D., & Smith, T. G. (1995). Melt blending of linear low-density polyethylene and polystyrene in a haake  
377 internal mixer. ii. Morphology-processing relationships. *Journal of Applied Polymer Science*, 58, 129-141.
- 378 Yang, Z., Gu, Q., Lam, E., Tian, F., Chaieb, S., & Hemar, Y. (2016a). In situ study starch gelatinization under ultra-high  
379 hydrostatic pressure using synchrotron saxs. *Food Hydrocolloids*, 56, 58-61.
- 380 Yang, Z., Swedlund, P., Hemar, Y., Mo, G., Wei, Y., Li, Z., & Wu, Z. (2016b). Effect of high hydrostatic pressure on the  
381 supramolecular structure of corn starch with different amylose contents. *International Journal of Biological*  
382 *Macromolecules*, 85, 604-614.
- 383 Yu, L., Dean, K., & Li, L. (2006). Polymer blends and composites from renewable resources. *Progress in Polymer Science*,  
384 31, 576-602.
- 385 Zhang, B., Chen, L., Xie, F., Li, X., Truss, R. W., Halley, P. J., Shamshina, J. L., Rogers, R. D., & McNally, T. (2015).  
386 Understanding the structural disorganization of starch in water-ionic liquid solutions. *Physical Chemistry*

- 387            *Chemical Physics*, 17, 13860-13871.
- 388    Zhang, J., Chen, F., Liu, F., & Wang, Z.-W. (2010). Study on structural changes of microwave heat-moisture treated
- 389            resistant canna edulis ker starch during digestion in vitro. *Food Hydrocolloids*, 24, 27-34.

390

391

392

**Tables and Figures**

Table 1 Degree of damaged starch granules (%) after kneading for different times.

Fig.1 Typical curve of torques vs. time measured by the Haake Rheomix mixer for G80

Fig. 2 SEC weight distributions of whole (fully-branched) starches after kneading for different times.

Fig. 3 SEC weight distributions of debranched maize starch after kneading for different times.

Fig. 4 Double-logarithmic SAXS patterns of corn starches after kneading for different times.

Fig.5 Porod SAXS patterns of corn starches after kneading for different times

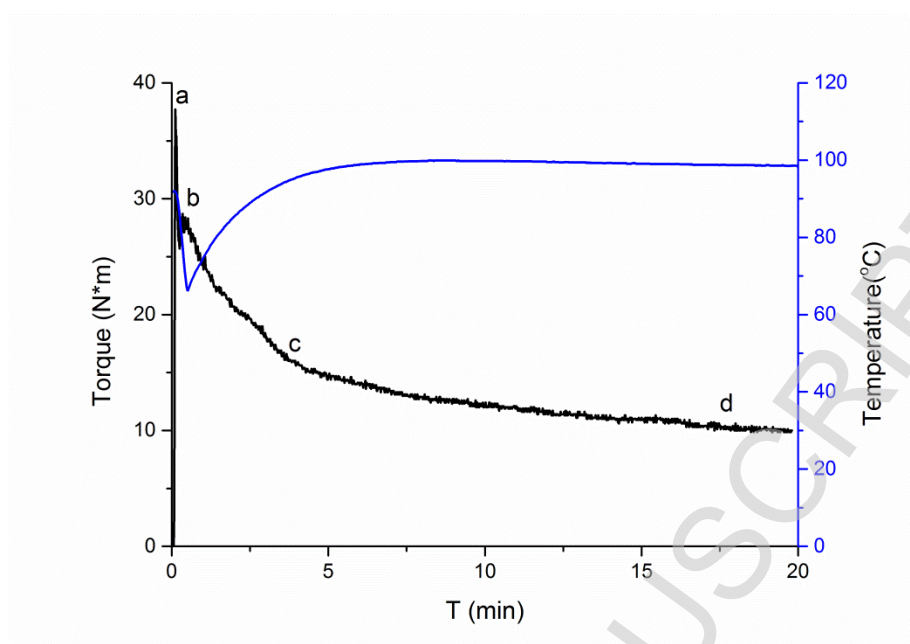


Fig.1 Typical curve of torques vs. time measured by the Haake Rheomix mixer for G80

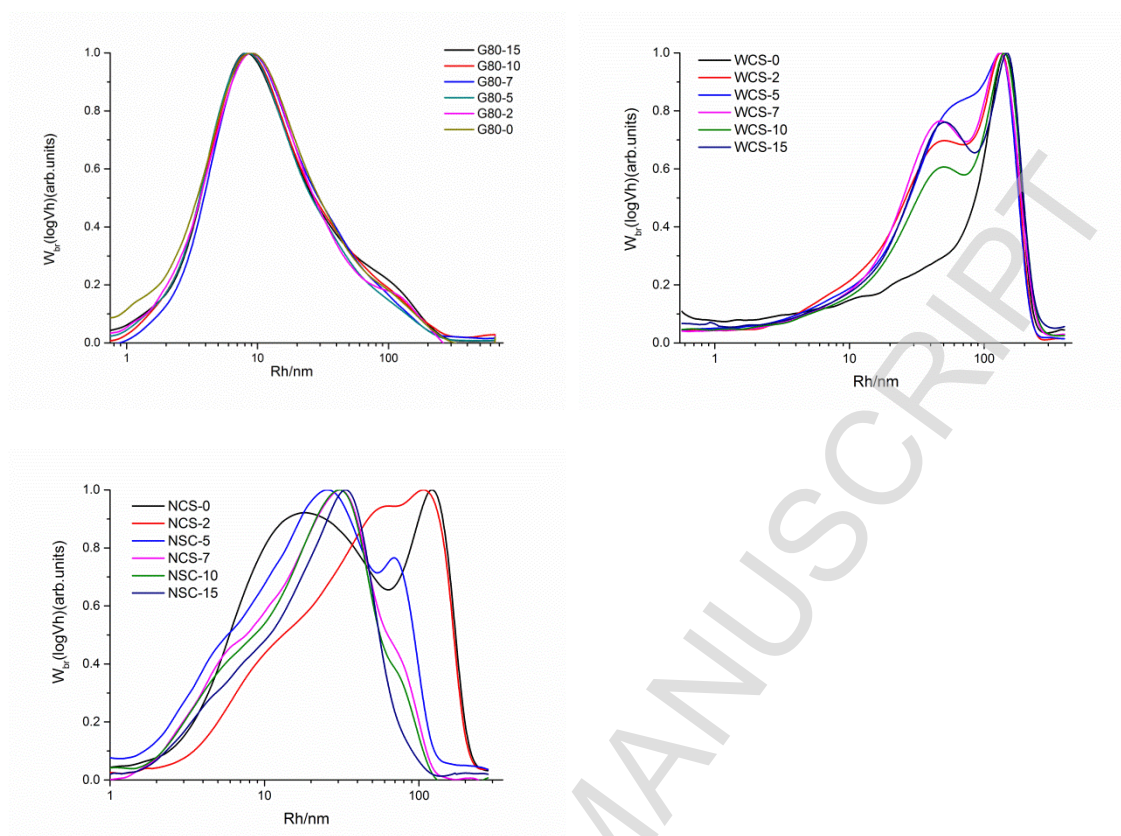


Fig. 2 SEC weight distributions of whole (fully-branched) starches after kneading for different times.



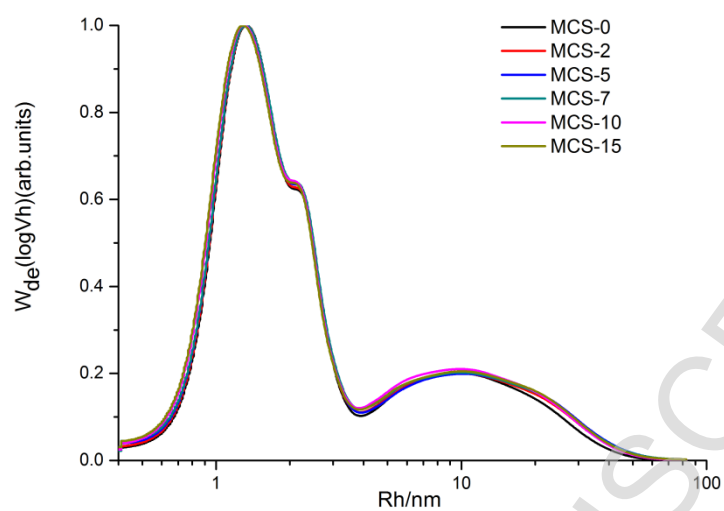


Fig. 3 SEC weight distributions of debranched maize starch after kneading for different times.

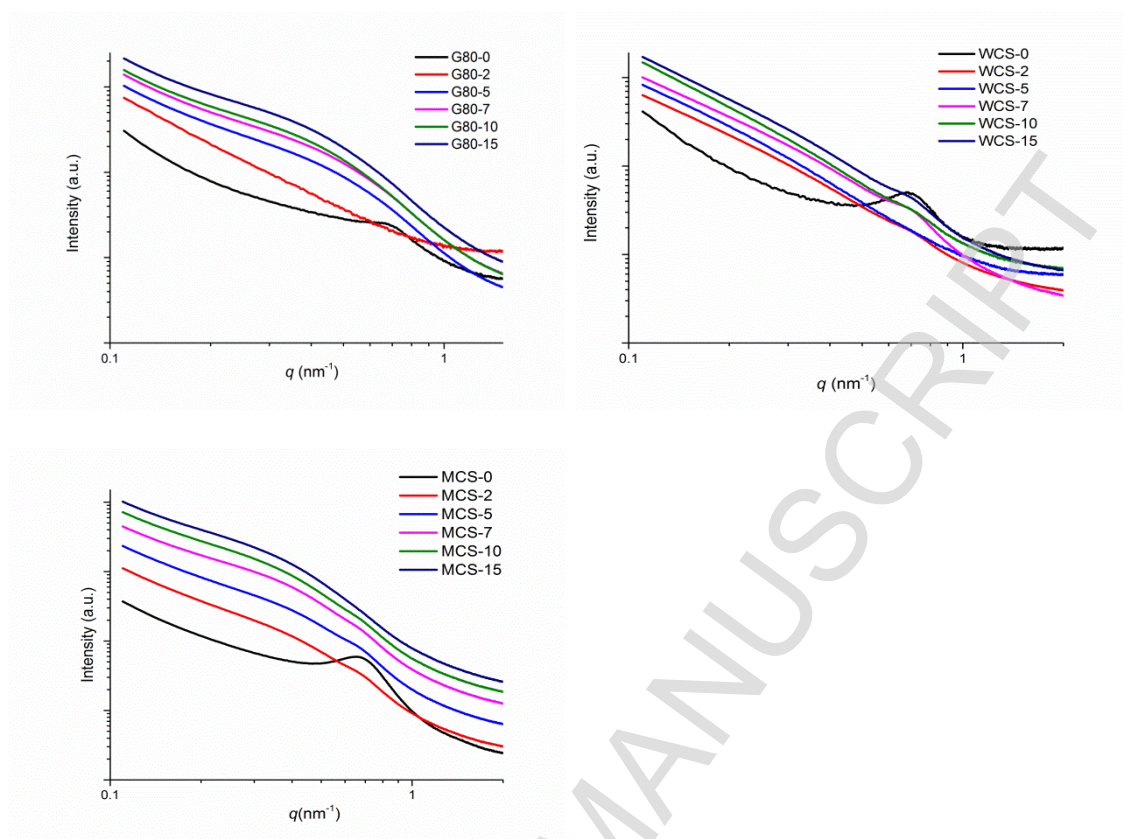


Fig.4 Double-logarithmic SAXS patterns of corn starches after kneading for different times.

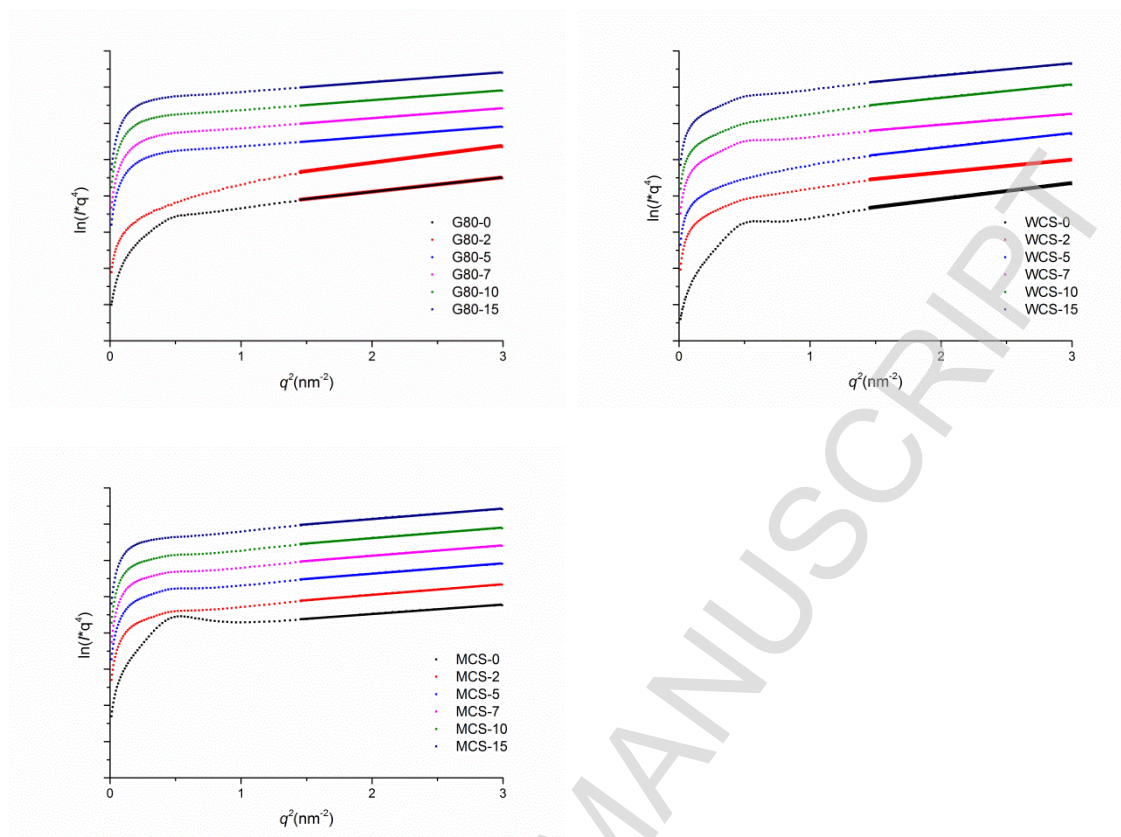


Fig.5 Porod SAXS patterns of corn starches after kneading for different times

Table 1 Degree of damaged starch granules (%) after kneading for different times.

Time (min)	WSC	NCS	G80
0	1.5±0.02	0.7±0.01	1.2±0.00
2	32.3±0.22	24.8±0.10	22.0±0.02
5	24.3±0.01	21.1±0.07	22.8±0.02
7	41.4±0.10	20.6±0.01	19.5±0.04
10	39.9±0.10	21.4±0.07	26.2±0.99
15	36.4±0.07	25.2±0.01	20.5±0.13